

Extraction of carrier transport parameters from hydrogenated amorphous and nanocrystalline silicon solar cells

Baojie Yan, Guozhen Yue, Laura Sivec, Jeffrey Yang, and Subhendu Guha

United Solar Ovonic LLC, 1100 West Maple Road, Troy, Michigan 48084

ABSTRACT

Transport properties are very important for solar cells. The efficiency of solar cells is determined by the competition of carrier collection and recombination. The most important parameter is the carrier mobility-lifetime product. However, methods commonly used for measuring transport parameters require specially designed samples. The results are often not easily correlated to solar cell performance. In this paper, we present our studies of extraction of material properties from conventional current-voltage characteristics and quantum efficiency curves. First, we carried out analyses of shunt resistance as a function of the light intensity. For solar cells with no clear parasitic shunt resistance, the shunt resistance is inversely proportional to the short-circuit current, and its proportionality coefficient is related to the effective carrier mobility-lifetime product. For an a-Si:H solar cell made under an optimized condition with high hydrogen dilution, the effective mobility-lifetime product was estimated to be $1.2 \times 10^{-8} \text{ cm}^2/\text{V}$. For a-SiGe:H solar cells, the effective mobility-lifetime product depends on Ge content. For optimized a-SiGe:H bottom cells used in high efficiency a-Si:H/a-SiGe:H/a-SiGe:H triple-junction structures, their values are $\sim 5.0 \times 10^{-9} \text{ cm}^2/\text{V}$. For high efficiency nc-Si:H solar cells, the effective mobility-lifetime product is $\sim 5.0 \times 10^{-7} \text{ cm}^2/\text{V}$. Second, we measured the quantum efficiency as a function of electrical bias and developed an analytical model to deduce the effective mobility-lifetime product. The results obtained from the second method are consistent with the values from the first method. We will present detailed analyses and interpretations of the transport parameters and their correlation to solar cell performance.

Key words: a-Si:H, nc-Si:H, solar cells, transport property, mobility-lifetime product.

1. INTRODUCTION

Hydrogenated amorphous silicon (a-Si:H), silicon-germanium alloy (a-SiGe:H), and nanocrystalline silicon (nc-Si:H) have been widely used in thin film solar cells because of the low cost and suitability for large volume mass production.¹ In recent years, multi-junction solar cells made with these materials have been improved by using nc-Si:H as an absorber layer in the bottom cell.²⁻⁶ In order to improve solar cell efficiency further, understanding the material properties is important. However, there is not always a direct correlation between material properties measured by specially designed characterization methods and solar cell performance.⁷ Recently, Schiff and his colleagues have studied the relation of material properties and solar cell performance using simulation and experimental methods. They found that the hole mobility (μ_h) is one of the dominant factors for determining the initial solar cell efficiency.^{8,9} The solar cell efficiency of an *n-i-p* (or *p-i-n*) structure is determined by the competition of extraction of the photo-generated carriers from the intrinsic layer by the built-in potential and their recombination through defects such as dangling bonds. Therefore, a rapid motion of photo-generated carriers out of the intrinsic layer and a low probability of recombination result in high solar cell efficiency. Because hole mobility is much lower than electron mobility in a-Si:H based materials, it is one of the limiting factors for a-Si:H based solar cell efficiency as shown by Schiff *et al.*^{8,9} On the other hand, a shorter carrier lifetime (τ), increases the chance of recombination and reduces a-Si:H solar cell performance. Evidence for this is that prolonged light-soaking creates metastable defects, which act as recombination centers and thus degrade the solar cell performance. This seems to make the hole mobility-lifetime ($\mu\tau$)_h product the dominant factor governing the solar cell efficiency. However, the amount of extracted photo-electrons and photo-holes must be equal during a steady state operation of a solar cell for maintaining a steady state charge distribution in the solar cell. Because of the unbalanced electron and hole mobility-lifetime products, electrons move out from the intrinsic layer easier than holes, if they experience

the same electric field. With consideration of the steady state charge distribution, and the unbalanced transport properties, one would expect to have non-uniform distribution of electric field, where it should be much stronger in the region near the p/i interface than in the region near the i/n interface. The non-uniform electric field and its correlation with the electron and hole mobilities were studied by simulation in the early 80's by Hack and Shur.¹⁰ The increased electric field by space charges in the p/i region enhances the hole extraction and the weakened electric field in the i/n region slows down the electron movements. Therefore, both the electron and hole mobility products are important for solar cell performance.

There are only a few methods to measure the carrier mobility, lifetime, and mobility-lifetime product in a-Si:H based materials. The time-of-flight method is commonly used for that purpose.¹¹⁻¹³ Here the carrier mobility is deduced from the transit time and the lifetime from the reduction of collected charge as a function of delayed time under different electric bias voltages. Unfortunately, for these measurements, one needs a relatively thick material to observe a clear transient time and a large charge collection without being significantly influenced by the displacement current from the geometric capacitance. Moreover, the a-Si:H based materials are typically non-uniform along the growth direction, especially for a-Si:H deposited close to the amorphous/nanocrystalline transition region.¹⁴ This issue is even more serious in nc-Si:H because the nanocrystallites grow with film thickness when a constant hydrogen dilution is used.¹⁵⁻¹⁷ Photoconductivity and steady-state photocurrent are two other useful methods to obtain carrier mobility-life products in a-Si:H based materials.^{18,19} However, both methods use co-planar sample structures and measure the electron lateral transport instead of the vertical transport in solar cells. For solar cell researchers, a simple method to extract the carrier transport properties from solar cells directly is very desirable, especially from the conventional measurement method such as current density versus voltage (J-V) characteristics and quantum efficiency curves. For this purpose, several methods had been proposed by different groups. In the early stage of a-Si:H based solar cell study, Crandall *et al.* measured the photocurrent as a function of bias voltage and determined the collection length of carriers in a-Si:H solar cells.²⁰⁻²⁴ He found a correlation between the collection length and fill factor (FF) in a-Si:H solar cells.²¹⁻²² He first used a uniform electric field approximation,²⁰ and then presented a non-uniform modeling.²³ In the late 90s, the groups of University of Neuchatel and University of Barcelona did a comprehensive analyses of the mobility-lifetime products in a-Si:H solar cells. They proposed effective mobility-lifetime product, which was proven to be a factor that has a clear correlation to the solar cell performance.²⁵⁻²⁷

In this paper, we first use a method proposed by Merten *et al.*²⁶ and Asensi *et al.*,²⁷ where the shunt resistance as a function of illumination density is used to deduce the effective carrier mobility-lifetime product. Second, we use a method similar to Crandall's approach,²¹ where the photocurrent as a function of bias voltage is measured and used to calculate the effective carrier mobility-lifetime product based on a new proposed analytical approach.

2. EXPERIMENTAL

Various $n-i-p$ solar cells made with RF and VHF glow discharges were characterized. The intrinsic layers include a-Si:H, a-SiGe:H, and nc-Si:H. Stainless steel (SS) and Ag/ZnO back reflector (BR) coated SS were used as substrates. Indium-Tin-Oxide (ITO) dots were deposited on the top of p layer as top transparent contacts. Light J-V characteristics were measured under an AM1.5 solar simulator at 25°C. QE curves were measured in the wavelength range between 300 to 1200 nm under the short-circuit condition, or under various electrical biases. For light intensity dependence of J-V characteristics, neutral density filters were used to vary the light intensity.

3. RESULTS AND DISCUSSION

3.1. Extraction of mobility-lifetime product from shunt resistance

Merten *et al.*²⁶ did an analysis of solar cell performance parameters and their correlations to transport properties. A correlation between the shunt resistance (R_{sh}) and short circuit current (I_{sc}) was deduced as,

$$R_{sh} = \frac{(\mu\tau)_{eff} V_b^2}{d^2} \times \frac{1}{I_{sc}}, \quad (1)$$

where V_{bi} is the built-in potential, d the thickness of the intrinsic layer, and $(\mu\tau)_{eff}$ the effective carrier mobility-lifetime product. The definition of $(\mu\tau)_{eff}$ is given by,

$$(\mu\tau)_{eff} = 2 \frac{(\mu_n^0 \tau_n^0)(\mu_p^0 \tau_p^0)}{\mu_n^0 \tau_n^0 + \mu_p^0 \tau_p^0}, \quad (2)$$

where μ_n^0 and μ_p^0 are the band mobilities of electrons and holes, respectively, and τ_n^0 and τ_p^0 are capture time of electrons and holes, respectively.²⁶⁻²⁷ If the parasitic shunt resistance is much larger than the internal shunt resistance, one can measure the J - V characteristics under different light intensities and plot the shunt resistance as a function of short-circuit current density (J_{sc}). From the slope of the R_{sh} versus $1/J_{sc}$, $(\mu\tau)_{eff}$ can be calculated if a linear relation is obtained.

We measured the J - V characteristics of many a-Si:H, a-SiGe:H, and nc-Si:H single-junction solar cells under different light intensities. Here, we present the results from two a-Si:H solar cells as an example. These two solar cells were deposited on SS using VHF glow discharge at high rates of 8-10 Å/s. The performance characteristics of these two solar cells are listed in Table I. Figure 1 plots (left) the J_{sc} versus light intensity and (right) the V_{oc} versus J_{sc} for the two a-Si:H solar cells, where one cell (18150) was deposited with high hydrogen (H-H) dilution and the other (18152) with low hydrogen dilution (L-H). The linear relation between J_{sc} and light intensity is because the photocurrent is a primary current. The different slopes of the two lines could result from two factors. First, the high hydrogen diluted cell is slightly thinner than the low diluted one; second the bandgap of the high hydrogen diluted one is slightly wider than that of the low hydrogen diluted one.²⁸ The linear relation between V_{oc} and $\ln(J_{sc})$ indicates that the superposition of the photocurrent and dark-current can still be used in a-Si:H solar cells as a first order of approximation although the photocurrent is a function of bias voltage and it is different under

Table I: J-V characteristics of various solar cells and the estimated effective carrier mobility lifetime products $(\mu\tau)_{eff}$. J_{sc} is the short-circuit current density, V_{oc} the open-circuit voltage, FF the fill factor, Eff the efficiency, and d the thickness of the intrinsic layer. H-H and L-H denote high hydrogen dilution and low hydrogen dilution, respectively.

Sample #	Type	Comments	J_{sc} (mA/cm ²)	V_{oc} (V)	FF	Eff (%)	d (nm)	V_{bi} (V)	$(\mu\tau)_{eff}$ (cm ² /V)
18150	a-Si:H	On SS, H-H	9.43	1.010	0.743	7.08	204	1.20	1.2×10^{-8}
18152	a-Si:H	On SS, L-H	10.04	0.971	0.605	5.90	228	1.17	8.3×10^{-9}
17067	a-SiGe:H	On SS, H-H	16.95	0.662	0.646	7.25	156	0.75	5.6×10^{-9}
17066	a-SiGe:H	On BR, H-H	23.11	0.668	0.617	9.52	156	0.75	5.0×10^{-9}
17076	nc-Si:H	On SS	16.86	0.545	0.671	6.16	1500	0.65	9.0×10^{-7}
17078	nc-Si:H	On BR	25.69	0.512	0.610	8.02	1500	0.65	5.7×10^{-7}

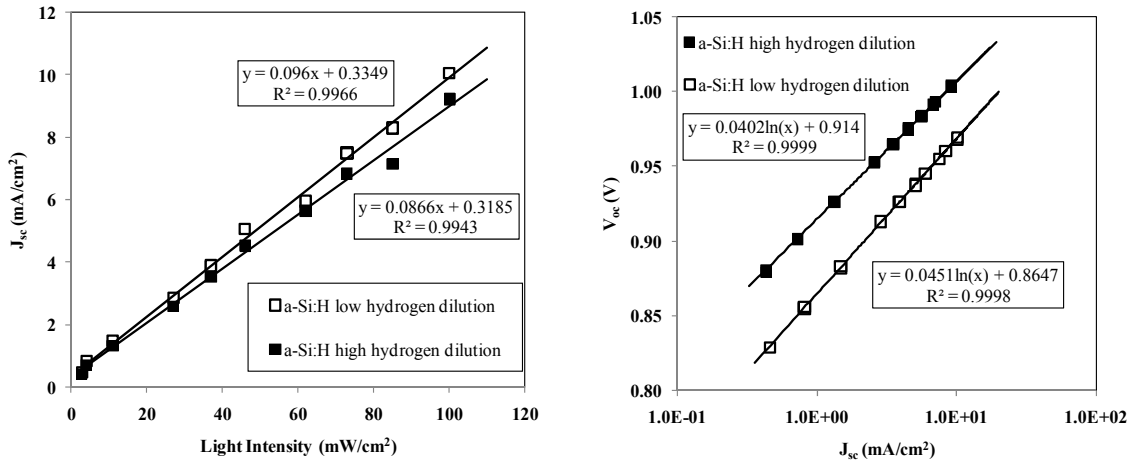


Figure 1. (left) J_{sc} versus light intensity and (right) V_{oc} versus J_{sc} for two a-Si:H solar cells on SS substrates, where one cell was deposited with high hydrogen dilution and the other with low hydrogen dilution.

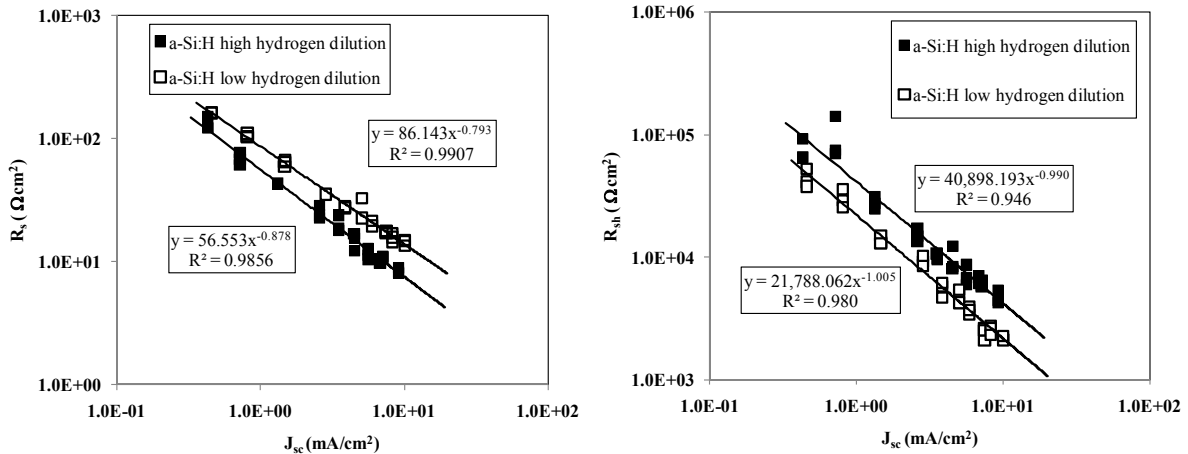


Figure 2. (left) R_s versus J_{sc} and (right) R_{sh} versus J_{sc} for the two a-Si:H solar cells as displayed in Fig. 1.

the open-circuit and short-circuit conditions. The slightly difference in the slopes is from the different quality factor (n); and the difference in the intersection is mainly from the saturated reverse current in the dark J-V characteristics.

Figure 2 plots the series resistance (R_s) and R_{sh} versus J_{sc} for the two a-Si:H solar cells shown in Fig. 1. Both R_s and R_{sh} show a linear relation in the double logarithmic plot. R_s is normally contributed by the internal resistance and the external resistance. The internal resistance is mainly from the resistance of the intrinsic layer, where the photoconductivity has a sub-linear relation with the light intensity. As pointed out in the previous paragraph, the photocurrent is a primary photocurrent in $n-i-p$ solar cells, where the photocurrent intensity is linearly proportional to the light intensity as shown in Fig. 1. Therefore, the sub-linearity of R_s versus J_{sc} reflects the light intensity dependence of photoconductivity of the intrinsic layer. The exponent should be related to the exponent of the conductivity versus light intensity, which should be 0.5 for bi-molecular recombination and 1.0 for mono-

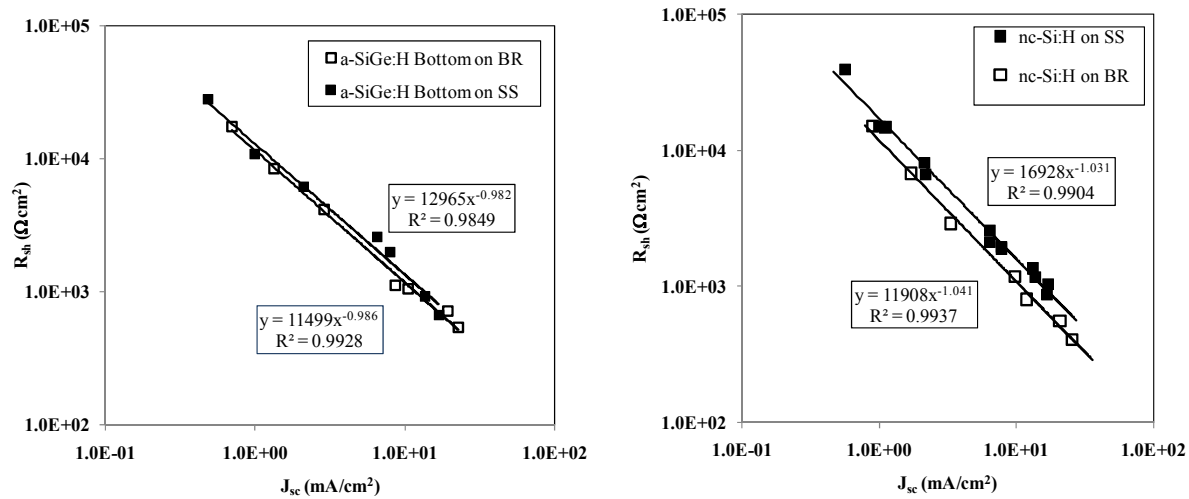


Figure 3. R_{sh} versus J_{sc} for (left) two a-SiGe:H bottom cells and (right) two nc-Si:H solar cells. In each pair, the deposition conditions were the same except for the different substrates.

molecular recombination. As shown in the left plot of Fig. 2, the exponent is around 0.8 for most solar cells studied in this paper. The most important result is the linear relation between R_{sh} and $1/J_{sc}$ as shown in the right plot of Fig. 2, where the exponent is very close to one within experimental errors. This result proves that $eq.(1)$ is applicable for $(\mu\tau)_{eff}$ estimation. The calculated $(\mu\tau)_{eff}$ values for the two a-Si:H solar cells made with high and low hydrogen dilution ratios are $1.8 \times 10^{-8} \text{ cm}^2/\text{V}$ and $8.3 \times 10^{-9} \text{ cm}^2/\text{V}$, respectively. The smaller $(\mu\tau)_{eff}$ in the low hydrogen diluted sample indicates a poorer material quality than the high hydrogen diluted sample. In the calculation, V_b is needed. However, we do not have accurate values for V_b in each sample. We assumed $V_b=1.20\text{V}$ for the high hydrogen diluted sample and 1.17 V for the low hydrogen diluted sample. Because of the uncertainty in V_b , the estimated $(\mu\tau)_{eff}$ might have a large error bar. We used the same method for a-SiGe:H and nc-Si:H solar cells. The performance characteristics of the a-SiGe:H and nc-Si:H solar cells are also listed in Table I. Figure 3 plots the R_{sh} versus J_{sc} for (left) one pair of a-SiGe:H solar cells and (right) one pair of nc-Si:H solar cells. For each pair, the deposition conditions were the same. The only difference was the substrates. For the a-SiGe:H solar cells, the $(\mu\tau)_{eff}$ values are $5.6 \times 10^{-9} \text{ cm}^2/\text{V}$ and $5.0 \times 10^{-9} \text{ cm}^2/\text{V}$, for the substrates of SS and Ag/ZnO BR, respectively. For the nc-Si:H solar cells, the corresponding values are $9.0 \times 10^{-7} \text{ cm}^2/\text{V}$ and $5.7 \times 10^{-7} \text{ cm}^2/\text{V}$, which are about two orders of magnitude larger than those of a-SiGe:H solar cells. The Ag/ZnO BR causes a reduction in the $(\mu\tau)_{eff}$ for both a-SiGe:H and nc-Si:H solar cells. As a result, the FF of solar cells on the Ag/ZnO BRs is poorer than that on SS. The difference becomes larger for nc-Si:H solar cells. Yue *et al.* did a systematic study and found the nc-Si:H material quality deteriorates with the textures of Ag/ZnO substrates. This is responsible for the low FF in nc-Si:H solar cells on Ag/ZnO BR.²⁹ The estimated $(\mu\tau)_{eff}$ values of nc-Si:H solar cells are consistent with the previous solar cell analysis.

For a-Si:H based solar cells, the FF is normally believed to be an indication of intrinsic material quality. Generally speaking, the FF depends on the light intensity, because the splitting of electron and hole quasi-Fermi levels increases with the light intensity. The defects between the two quasi-Fermi levels are recombination centers for photo-generated carriers. Therefore, if the cell performance is limited by deep defects in the intrinsic layer, one would observe a strong light intensity dependence of FF. If the cell performance shows a weak light intensity dependence, the cell performance may not be limited by deep defects. In this case, the cell performance could be limited by the band tails as proposed by Schiff *et al.*⁹ The left plot in Fig. 4 shows FF as a function of J_{sc} . One can see that the a-Si:H solar cell deposited with high hydrogen dilution has a very weak light intensity dependent FF, indicating a low defect density; while the a-Si:H solar cell deposited with low hydrogen dilution has a strong light intensity dependence of FF, indicating a high defect density. With a simplified mind, the FF of a solar cell shall

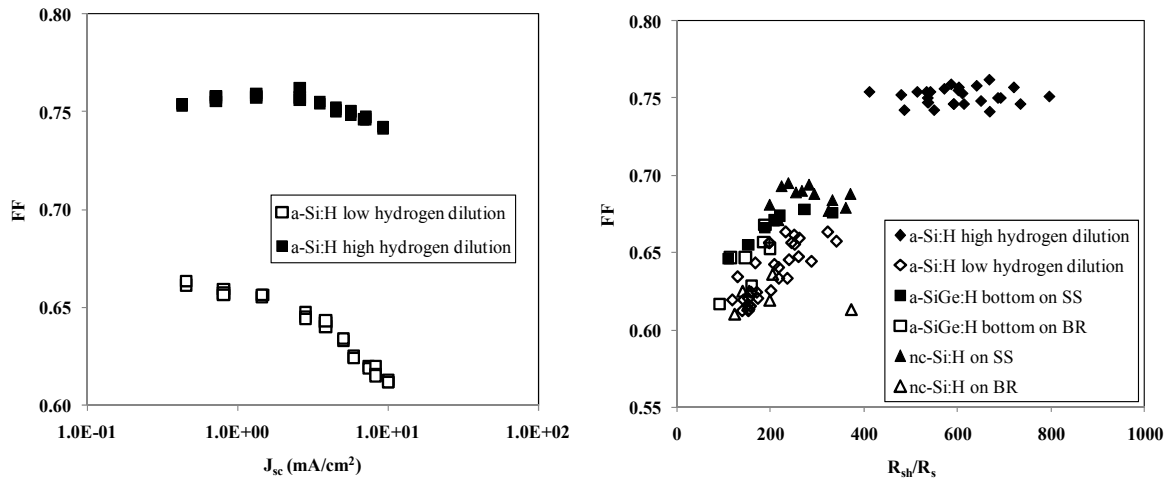


Figure 4. (left) FF as a function of J_{sc} for the two a-Si:H solar cells shown in Figs. 1 and 2. (right) FF versus R_{sh}/R_s for all solar cells listed in Table I.

have a strong relation with the R_s and R_{sh} as well. The R_s determines the sharpness of the J-V curve at the open-circuit condition and the R_{sh} reflects the flatness of J-V curve at the short circuit condition. The smaller the R_s and the larger the R_{sh} , the better the FF should be. Therefore, we would like to investigate whether this predication is generally true or not. As a test, we show the FF as a function of R_{sh}/R_s on the right plot of Fig. 4 for various solar cells. For most of the solar cells, the FF increases with the increase of R_{sh}/R_s , except for the a-Si:H and nc-Si:H solar cells on SS substrates. For these two solar cells, the FF does not show a clear correlation with the R_{sh}/R_s . The FF values are very high in these two solar cells. It appears that the effective series resistance and shunt resistance are no longer the limiting factor for the FF. A more careful analysis in this regime is in process. One hypothesis is that the FF in these good solar cells is not limited by the recombination through defects. The bandtail recombination could be the dominant factor.

3.2. Extraction of mobility-lifetime product from biased quantum efficiency

Similar to the attempt by Crandall *et al.*,^{21,22} we describe an estimation method to extract the $(\mu\tau)_{eff}$ from the light J-V characteristic under weak illumination, which we measured using our quantum efficiency setup. First, we present the physical basis of the method. Considering an a-Si:H solar cell with an *n-i-p* structure under illumination, the carrier densities (both free carriers and trapped carriers) and current densities are normally calculated by solving Poisson's equation and carrier continuity equations as described by Hack and Shur.¹⁰ However, the calculation is complicated and results are not very straightforward to be used by solar cell researchers. Here we provide a simplified approach.

Under illumination, carrier generation in a solar cell is a function of its location in the *i* layer, noted as $G(x)$. The electron and hole densities are also functions of locations, noted as $n(x)$ and $p(x)$. For simplicity, we use the average carrier densities (n and p) and average generation rate (G). In the steady state, we assume the average electron and hole densities are equal in the *i* layer. Therefore, we are dealing with one type of carrier only. The average electron density shall satisfy the following equation,

$$\frac{dn}{dt} = G - \frac{n}{\tau} - \frac{n}{t_{ex}}, \quad (3)$$

where τ is the carrier lifetime and t_{ex} the extract time of carriers from the intrinsic layer. For simplicity, t_{ex} could be the average transit time (t_T) of carriers moving out of the i layer. It is well known that electrons and holes have different mobilities, therefore, the extraction time for electrons and holes could be different. However, in the steady state condition, the charge distribution in the intrinsic layer creates an electric field distribution such that it is much stronger in the p/i interface. The non-uniform electric field accelerates the movement of holes and slows down the movement of electrons. As a net result, the amount of electrons and holes moving out of the device must be equal. Therefore, the extraction time of electrons and holes must be equal as well. In addition, the amounts of electrons and holes lost through recombination are the same. Therefore, the lifetimes of electrons and holes must be equal as well, even though the real mobilities and lifetimes measured by conventional methods are different for electrons and holes. In this case, we use effective mobility similar as discussed in the previous section. Logically speaking, the extraction time shall be proportional to the thickness (d) of the i layer and inversely proportional to the average electric field (E) and effective carrier mobility (μ_{eff}). We define the extraction time as an average transit time $t_{ex}=d/(\mu_{eff}E)$. We assume the average electric field $E=(V_a+V_{bi})/d$, where V_a is the magnitude of reverse bias voltage and V_{bi} the built-in potential. We define an effective lifetime τ_{eff} ,

$$\tau_{eff} = \frac{\tau_{eff} t_T}{\tau_{eff} + t_T}, \quad (4)$$

to describe the time that carriers stay in the i layer before they recombine or are extracted. In a steady state, Eq. (3) becomes

$$n = G \tau_{eff} = G \frac{\tau_{eff} t_T}{\tau_{eff} + t_T} = G \frac{\tau_{eff} d}{(\mu\tau)_{eff} E + d}. \quad (5)$$

In this case, we assume that the current density is proportional to carrier density and effective mobility, then $J=qn\mu_{eff}E$. Using Eq. (5) with $E=(V_a+V_b)/L$, we obtain

$$J = qGL \frac{(\mu\tau)_{eff} (V_a + V_b)}{(\mu\tau)_{eff} (V_a + V_b) + d^2}. \quad (6)$$

For a positive bias, the sign of V_a is negative.

Fitting the photocurrent density as a function of applied voltage to Eq. (6) yields $(\mu\tau)_{eff}$. There are two limiting cases for Eq. (4). The first is that when a very high reverse bias is applied, such that $(\mu\tau)_{eff}(V_a+V_b)$ is much larger than d^2 , then the current $J=qGd$ does not depend on the bias voltage, indicating a generation limited photocurrent. Second, when the applied voltage is close to the built-in potential, the current is close to zero (open-circuit). Under this condition, the electric field is very weak for carrier collection.

We use a conventional QE setup to measure the current density by integrating the measured QE values with the AM1.5 solar spectrum. Because the QE curves were measured with a lock-in method using a low chopping frequency (~ 30 Hz), the influence of the dark current and of the transient response were minimized. Let $Q(V_a)$ denote the $J(V_a)$ measured under a bias of V_a from the QE setup and normalize the data to a fixed bias V_0 (say -1.0 V), then,

$$\frac{Q(V_a)}{Q_0(V_0)} = \frac{(V_a + V_b) \{(\mu\tau)_{eff} (V_0 + V_b) + d^2\}}{(V_0 + V_b) \{(\mu\tau)_{eff} (V_a + V_b) + d^2\}}. \quad (7)$$

Experimentally, we measured the QE curves under various biases and calculated the current density with a built-in function of the measurement system. Then, we fit the measured data with Eq. (7) to obtain the effective mobility-lifetime $(\mu\tau)_{eff}$ product and the built-in potential (V_b).

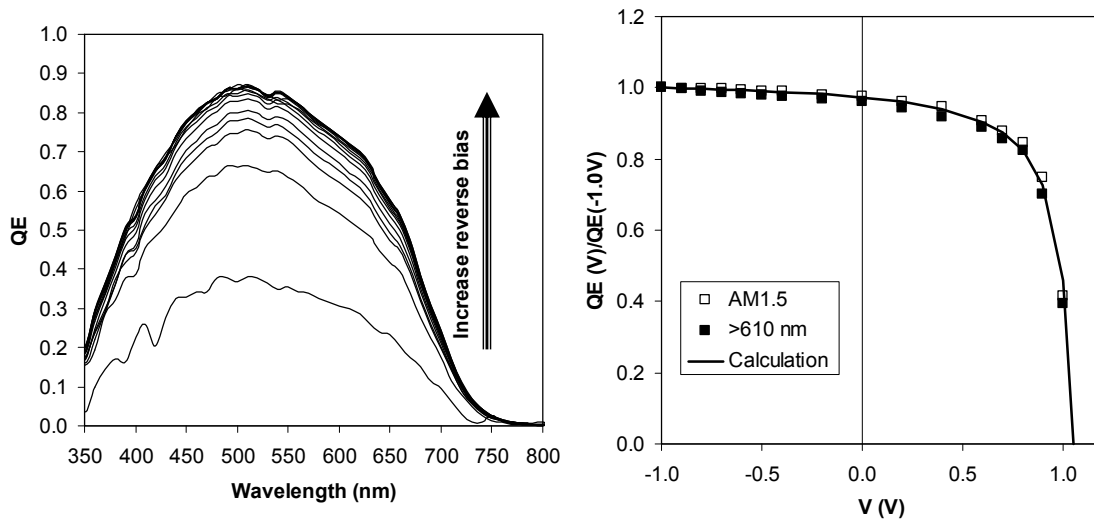


Figure 5. Quantum efficiency, QE, as a function of light wavelength of an a-Si:H solar cell measured under various electrical biases. From the bottom curve to the top, the electrical bias changes from +1.0 to -1.0V.

Table II: Solar cell performance characteristics and corresponding effective mobility-lifetime products and average built-in potential (V_{bi}). J_{sc} is the short-circuit current density, V_{oc} the open-circuit voltage, FF the fill factor, and η the efficiency. d is the thickness of the intrinsic layer.

Sample #	Type	J_{sc} (mA/cm ²)	V_{oc} (V)	FF	η (%)	d (nm)	V_{bi} (V)	$(\mu\tau)_{eff}$ (cm ² /V)
16677	a-Si:H on BR	14.03	1.009	0.693	9.81	220	1.05	8.0×10^{-9}
17066	a-SiGe:H on BR	23.11	0.668	0.617	9.52	156	0.70	3.1×10^{-9}
16413	a-SiGe:H on BR	24.55	0.686	0.618	10.40	170	0.72	4.0×10^{-9}
15454	nc-Si:H on BR	27.69	0.529	0.632	9.26	1500	0.60	6.4×10^{-7}

We measured several a-Si:H, a-SiGe:H, and nc-Si:H single-junction solar cells deposited on Ag/ZnO BR coated SS. Because the back reflector enhances the light trapping effect, the long wavelength light can travel many paths in the intrinsic layer. Therefore, the uniform absorption approximation is close to the real situation for long wavelength illumination. Table II lists the cell performance parameters, calculated $(\mu\tau)_{eff}$ product, and V_{bi} values. Figure 5 shows (left) an example of QE curves measured under different electrical biases ranging from +1.0 V to -1.0 V. The bottom curve corresponds to +1.0 V. The QE curves increase with increasing negative bias until they change and saturate. This implies a generation rate limited photocurrent. Figure 5 also shows (right) the normalized current as a function of applied bias for the a-Si:H solar cell shown in the left plot, where the open squares are data obtained from the entire AM1.5 spectrum, while the solid squares are only from the long wavelength (>610 nm) region of the AM1.5 spectrum. Essentially, the long wavelength data are lower than the entire spectrum data. This is because under a white light illumination, the short wavelength light generates electron-hole pairs close to the p/i interface, and under which condition, the photo-generated holes travel a shorter distance than those generated by

long wavelength photons. Therefore, the short wavelength generated holes are easier to collect than those generated by long wavelength photons. The solid line in the Fig. 1 is calculated from Eq. (7) with the parameters $(\mu\tau)_{eff}=8.0\times 10^{-9}$ cm²/V and $V_b=1.05$ V. This $(\mu\tau)_{eff}$ value is very close to the values obtained in the previous section. The V_{bi} is close to the open-circuit voltage (V_{oc}) and smaller than that used in the previous section. The smaller V_b in this calculation is believed to be due to the non-uniform distribution of the electric field, which results in a weak field region. When the electric field in the weak field region is reduced to zero by an applied voltage, the photo-current will drop to zero. Therefore, the V_b obtained by this method should be smaller than the real V_b generated by the different Fermi levels in the doped layers.

We also determined the hole $(\mu\tau)_{eff}$ product in a-SiGe:H and nc-Si:H solar cells. Figure 6 shows (top) the QE curves of a nc-Si:H solar cell measured under various electrical biases and (bottom) the normalized long wavelength QE current as a function of electrical bias, respectively. By fitting the experimental data, we obtained $\mu\tau$ of 5.0×10^{-7} cm²/V, which is significantly larger than the value in the a-Si:H and a-SiGe:H solar cells as listed in Table II. The hole drift mobility of nc-Si:H measured by the time-of-flight method is around 1.0 cm²/Vs,³⁰ which is about 2 orders of magnitude larger than that in a-Si:H. Our measurements show that the $(\mu\tau)_{eff}$ product is about 80 times larger in the nc-Si:H cell than in the a-Si:H cell. It appears that the major increase in the $(\mu\tau)_{eff}$ products from a-Si:H to nc-Si:H is from the enhancement of the hole drift mobility. One can consider that nc-Si:H is a mixture of nanocrystalline phase, amorphous tissues, and grain boundaries. The carrier transport mainly takes place in the crystalline phase, because the carrier mobility in c-Si is much larger than in a-Si:H. This explains the enhanced drift mobility in nc-Si:H. However, the grain boundaries and amorphous tissues cause bond angle and bond length distortions and lead to defects and band tail states. Consequently, both the carrier mobility and the lifetime are lower in nc-Si:H than in c-Si.

Schiff and his colleagues have extensively studied the carrier transport in a-Si:H and nc-Si:H materials and solar cells

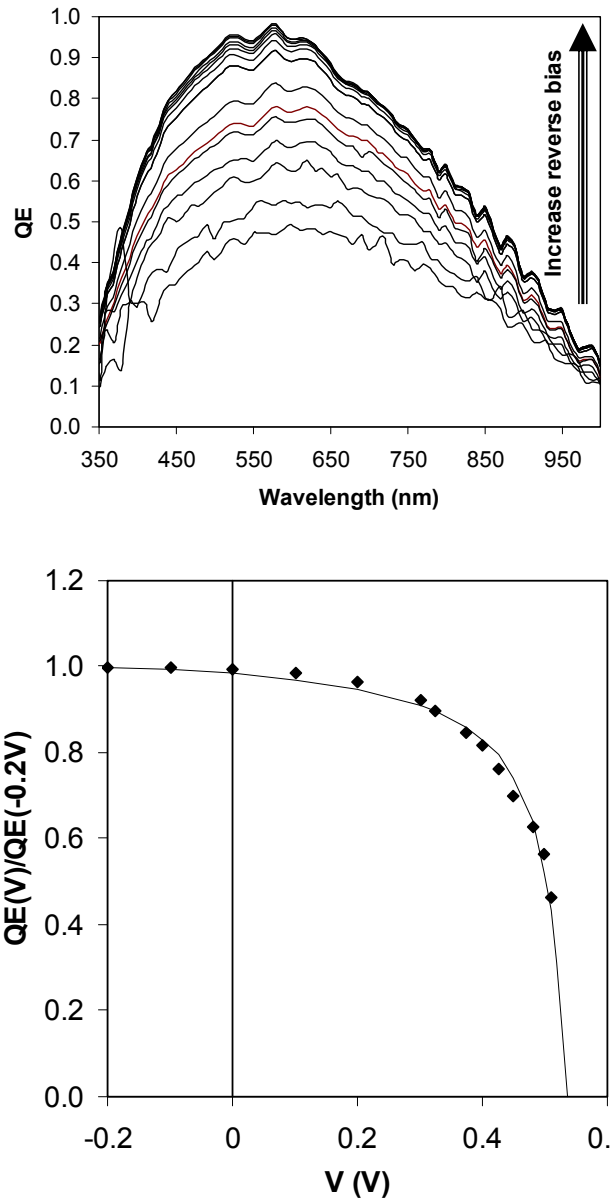


Figure 6. (top) QE curves of a nc-Si:H solar cell measured under various electrical biases. From the bottom curve to the top, the electrical bias changes from +0.5V to -1.0V. (bottom) normalized (to -0.2V) long wavelength (>610 nm) QE current density as a function of bias voltage for the nc-Si:H solar cell. The solid symbols are the measurement data and the solid line is calculated based on $(\mu\tau)_{eff}$ product of 6.4×10^{-7} cm²/V.

both theoretically and experimentally.^{8,9} Their conclusion is that the solar cell efficiency in a-Si:H based solar cells is mainly limited by the hole mobility. However, we believe that the solar cell efficiency should be limited by the effective carrier mobility-lifetime product because the carrier collection by the external circuit is the result of competition between the drift and recombination. The longer the lifetime and the faster the carriers move, the lower the probability that photo-carriers are lost via recombination. In addition, both electron and hole transport contributes to the carrier collection. A large difference in the electron and hole mobility generates a high non-uniform electric field, which accelerates the hole movements and slows down the electron movements. Therefore, the effective carrier mobility-lifetime product is the most important parameter for the solar cell performance. Any one carrier transport parameter only may not necessarily be the dominant factor for limiting the solar cell performance. Therefore, the lack of correlation between one single material property and solar cell efficiency is not surprising.

4. SUMMARY

The effective carrier mobility-lifetime products in a-Si:H, a-SiGe:H, and nc-Si:H solar cells are estimated by the shunt resistance as a function of the light intensity. The effective carrier mobility-lifetime product includes the transport properties of both electrons and holes because the same amount of electrons and holes should be collected by the external circuit. The experimental results are reasonably good and show a correlation with the material quality and solar cell performance. As reported in the literature, the electron mobility is much larger than the hole mobility. The un-balanced electron and hole mobilities creates non-uniform electric field distribution in the intrinsic layer, which accelerates the hole movement and slows down the electrons. Therefore, the solar cell performance is determined by both types of carriers. We also developed a method to deduce the effective carrier mobility-lifetime product by fitting the photocurrent as a function of voltage. A new analytical approach is introduced. Using this method, we have also studied a-Si:H, a-SiGe:H, and nc-Si:H solar cells. In general, the two methods give similar results.

ACKNOWLEDGMENTS

We thank the Research and Development team at United Solar Ovonic for their collaboration and assistance. This work has been supported by US DOE under SAI Program contract No. DE-FC36-07 GO 17053.

REFERENCES

- [1] Deb, S. K., "Recent Advances and Future Opportunities for thin-film solar cells" in [Thin-Film Solar Cells-Next Generation Photovoltaics and Its Applications], edited by Hamakawa, Springer, Berlin, 15-42 (2004).
- [2] Meier, J., Flückiger, R., Keppner, H., and Shah, A., "Complete microcrystalline *p-i-n* solar cell-crystalline or amorphous cell behavior?", Appl. Phys. Lett., 65(7), 860-862 (1994).
- [3] Shah, A.V., Meier, J., Vallat-Sauvain, E., Wyrsh, N., Kroll, U., Droz, C., and Graf, U., "Material and solar cell research in microcrystalline silicon", Sol. Energy Mater. & Sol. Cells, 78(1), 469-491 (2003).
- [4] Yan, B., Yue, G., and Guha, S., "Status of nc-Si:H solar cells at United Solar and roadmap for manufacturing a-Si:H and nc-Si:H based solar panels", Mater. Res. Soc. Symp. Proc., 989, 335-346 (2007).
- [5] Fukuda, S., Yamamoto, K., Nakajima, A., Yoshimi, M., Sawada, T., Suezaki, T., Ichikawa, M., Koi, Y., Goto, M., Meguro, T., Matsuda, T., Sasaki, T., and Tawada, Y., "High efficiency thin film silicon hybrid cell and module with newly developed interlayer", in [Proc. of 21st European Photovoltaic Solar Energy Conference], 1535-1538 (2006).
- [6] Takatsuka, H., Yamauchi, Y., Fukagawa, M., Mashima, H., Kawamura, K., Yamaguchi, K., Nishimiya, K., and Takeuchi, Y., "High efficiency thin film solar modules", in [Proc. 21st European Photovoltaic Solar Energy Conference], 1531-1534 (2006).
- [7] Xu, X., Yang, J., and Guha, S., "On the lack of correlation between film properties and solar cell performance of amorphous silicon-germanium alloys", Appl. Phys. Lett., 62(12), 1399-1401 (1993).
- [8] Liang, J., Schiff, E. A., Guha, S., Yan, B., and Yang, J., "Hole-mobility limit of amorphous silicon solar cells", Appl. Phys. Lett., 88(6), 063512 (2006)

- [9] Schiff, E.A., "Hole mobilities and the physics of amorphous silicon solar cells", *J. Non-Cryst. Solids*, 352(9), 1087-1092 (2006)
- [10] Hack, M. and Shur, M., "Physics of amorphous silicon alloy *p-i-n* solar cells", *J. Appl. Phys.*, 58(2), 997-1020 (1985).
- [11] Tiedje, T., "Information about band-tail states from time-of flight experiments", in [Semiconductors and Semimetals], 21C, edited by Pankove J. I., Academic Press, Inc, Orlando, 207-238 (1984).
- [12] Antoniadis, H. and Schiff, E. A., "Transient photocharge measurements and electron emission from deep levels in undoped a-Si:H", *Phys. Rev. B*, 46(15), 9482 (1992).
- [13] Gu, Q., Wang, Q., Schiff, E. A., Li, Y.-M., and Malone, C. T., "Hole drift mobility measurements in amorphous silicon-carbon alloys", *J. Appl. Phys.*, 76(4), 2310-2315 (1994).
- [14] Guha, S., Yang, J., Williamson, D. L., Lubianiker, Y., Cohen, J. D., and Mahan, A. H., "Structural, defect, and device behavior of hydrogenated amorphous Si near and above the onset of microcrystallinity", *Appl. Phys. Lett.*, 74(13), 1860 (1999).
- [15] Yan, B., Yue, G., Yang, J., Guha, S., Williamson, D. L., Han, D., and Jiang, C.-S., "Hydrogen dilution profiling for hydrogenated microcrystalline silicon solar cells", *Appl. Phys. Lett.*, 85(11), 1955-1957 (2004).
- [16] Bailat, J., Vallat-Sauvain, E., Feitknecht, L., Droz, C., and Shah, A., "Influence of substrate on the microstructure of microcrystalline silicon layers and cells", *J. Non-Cryst. Solids*, 299(2), 1219-1223 (2002).
- [17] Finger, F., Klein, S., Dylla, T., Baia Neto, A. L., Vetterl, O., and Carius, R., "Defects in microcrystalline silicon with hot wire CVD", *Mater. Res. Soc. Symp. Proc.*, 715, 123 (2002).
- [18] Crandall, R. S., "Photoconductivity", in [Semiconductors and Semimetals], 21B, edited by Pankove J. I., Academic Press, Inc, Orlando, 245-297 (1984).
- [19] Ritter, D., Weiser, K., and Zeldov, E., *J. Appl. Phys.* 62(11), "Steady-state photocarrier grating technique for diffusion-length measurement in semiconductors: Theory and experimental results for amorphous silicon and semi-insulating GaAs", *J. Appl. Phys.*, 62(11), 4563-4570 (1987).
- [20] Crandall, R. S., "Transport in hydrogenated amorphous silicon *p-i-n* solar cells", *J. Appl. Phys.*, 53(4), 3350-3352 (1982).
- [21] Faughnan, B. W. and Crandall, R. S., "Determination of carrier collection length and prediction of fill factor in amorphous silicon solar cells", *Appl. Phys. Lett.*, 44(5), 537-539 (1984).
- [22] Faughnan, B. W., Moore, A., and Crandall, R. S., "Relationship between collection length and diffusion length in amorphous silicon", *Appl. Phys. Lett.*, 44(6), 613-615 (1984).
- [23] Crandall, R. S., "Modeling of thin-film solar cells: Nonuniform field", *J. Appl. Phys.*, 55(12), 4418-4425 (1984).
- [24] Crandall, S. R., and Balberg, I., "Mobility-lifetime products in hydrogenated amorphous silicon", *Appl. Phys. Lett.*, 58(5), 508-510 (1991).
- [25] Beck, N., Wyrsh, N., Hof, Ch., and Shah, A., "Mobility lifetime product-A tool for correlating a-Si:H film properties and solar cell performances", *J. Appl. Phys.*, 79(12), 9361-9368 (1996).
- [26] Merten, J., Asensi, J. M., Voz, C., Shah, A. V., Platz, R., and Andreu, J., "Improved equivalent circuit and analytical model for amorphous silicon solar cells and modules", *IEEE Transactions on Electron Devices*, 45(2), 423-429 (1998).
- [27] Asensi, J. M., Merten, J., Voz, C., and Andreu, "Analysis of role of mobility-lifetime products in the performance of amorphous silicon solar cells", *J. Appl. Phys.*, 85(5), 2939-2951 (1999).
- [28] Yan, B., Yang, J., and Guha, S., "Effect of hydrogen dilution on the open-circuit voltage of hydrogenated amorphous silicon solar cells" *Appl. Phys. Lett.*, 83, 782-784 (2003).
- [29] Yue, G., Sivec, L., Yan, B., Yang, J., and Guha, S., "High efficiency amorphous and nanocrystalline based multi-junction solar cells deposited at high rates on textured Ag/ZnO back reflectors", *Mater. Res. Soc. Symp. Proc.*, 1153, A10-5 (2009).
- [30] Dylla, T., Finger, F., and Schiff, E. A., "Hole drift-mobility measurements in microcrystalline silicon", *Appl. Phys. Lett.*, 87(3), 032103 (2005).